Direct-Space Structure Determination of Covalent Organic Frameworks from 3D Electron Diffraction Data

Tu Sun[+], Colan E. Hughes[+], Linshuo Guo, Lei Wei, Kenneth D. M. Harris,* Yue-Biao Zhang,* and Yanhang Ma*

Abstract: Structure determination of covalent organic frameworks (COFs) with atomic precision is a bottleneck that hinders the development of COF chemistry. Although three-dimensional electron diffraction (3D-ED) data has been used to solve structures of sub-micrometer-sized COFs, successful structure solution is not guaranteed as the data resolution is usually low. We demonstrate that the direct-space strategy for structure solution, implemented using a genetic algorithm (GA), is a successful approach for structure determination of COF-300 from 3D-ED data. Structural models with different geometric constraints were considered in the GA calculations, with successful structure solution achieved from room-temperature 3D-ED data with a resolution as low as ca. 3.78 &. The generality of this strategy was further verified for different phases of COF-300. This study demonstrates a viable strategy for structure solution of COF materials from 3D-ED data of limited resolution, which may facilitate the discovery of new COF materials in the future.

Introduction

Covalent organic frameworks (COFs) are constructed from well-designed organic building blocks through covalent bonds, leading to extended 2D or 3D networks.[1] To date, COF chemistry has shown versatility of covalent linkages[2] and diversity of pore engineering,[3] leading to a range of functional applications.[4] While there is considerable scope for synthesis of new COFs, rigorous structural character-ization is a bottleneck in the development of this field. While single-crystal X-ray diffraction (SCXRD) studies have been reported[5] for a few COFs, this technique requires a single crystal sample of sufficient size and quality; however, due to synthetic limitations, most COFs are formed as microcrystal-line materials of low-crystallinity that are unsuitable for study by SCXRD. Instead, with knowledge of reticular chemistry, model building strategies coupled with powder X-ray diffrac-tion (PXRD) pattern-matching methods have often been used to elucidate COF structures.[1c, 6] In this approach, structural insights derived from other techniques such as FT-IR spectroscopy, solid-state NMR and gas/vapor sorption are often required. However, when the PXRD data has a low number of reflections and significant peak overlap, this strategy may be limited by uncertainty in the unit cell, space group, interpenetration number and dynamic properties of the COF material.

Electron diffraction provides an important alternative opportunity for structural characterization of materials.[7] The 3D-ED approach[8] has advanced rapidly for structure determination of framework materials,[9] small organic molecules (including pharmaceuticals),[10] macromolecules and proteins.[11] As electrons interact with matter about 10^3 to 10^4 times more strongly than X-rays, electron diffraction is superior for determining structures of nanocrystals, which are sufficiently large to give adequate electron diffraction data. In the development of COF chemistry, 3D-ED has played an important role in structure determination,[12] and structure solution of several COFs has been achieved from high-resolution 3D-ED data by traditional direct methods or charge-flipping algorithms.[12f,g,i] To achieve structure solution with a limited number of reflections, a simulated annealing (SA) method[13] was used on COF-320 and COF-300 using 3D-ED data with resolution 1.5 & and 1.65 & respective-ly.[12a,b] Recently, cryo-electron diffraction tomography (cryo-EDT) has also been developed to study the dynamic behavior of COFs and to locate guest molecules in sub-micrometer-sized COFs at the atomic level.[12g] However, there are no reports of successful structure solution of COFs achieved directly from 3D-ED data with resolution lower than 1.65 &.

Herein, we demonstrate the application of the direct-space strategy,[14] implemented using a genetic algorithm[15] (GA), for structure solution of COF materials of known structure (specifically, activated and hydrated forms of COF-300[16]) from low-resolution 3D-ED data (Figure 1) using the program EAGER,[17, 18] which was originally developed for direct-space structure solution from PXRD data. Based on knowledge of reticular chemistry and structural information obtained from the 3D-ED data, three distinct models were designed for the GA structure-solution calculations, each based on a specific definition of the structural fragment in direct space. We show that the direct-space GA strategy allows high-quality structure solution to be achieved from 3D-ED data with resolution as low as 3.78 &. Furthermore, three

[*] T. Sun,[+] L. Guo, L. Wei, Prof. K. D. M. Harris, Prof. Y. Zhang, Prof. Y. Ma
School of Physical Science and Technology, ShanghaiTech University Shanghai 201210 (P. R. China)
E-mail: zhangyb@shanghaitech.edu.cn
mayh2@shanghaitech.edu.cn
Dr. C. E. Hughes,[+] Prof. K. D. M. Harris School of Chemistry, Cardiff University Cardiff CF10 3AT (UK)
E-mail: HarrisKDM@cardiff.ac.uk
[+] These authors contributed equally to this work.

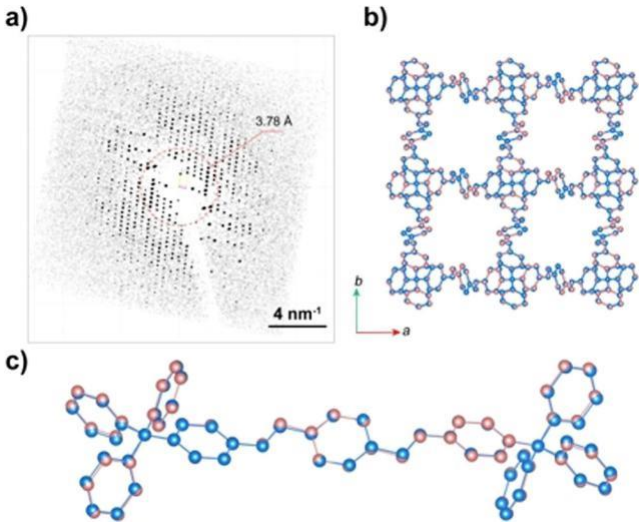

Figure 1. a) Projection of a reconstructed 3D reciprocal lattice along a random direction from the 3D-ED dataset COF-300-V-RT (the red circle indicates data at 3.78 & resolution). b) Overlay of the structure solution from direct-space GA calculations using the 3D-ED data at 3.78 & resolution (red) and the reported structure (blue).[12g] c) Overlay of individual fragments from (b). Geometric details are given in Tables S1 and S20.

different 3D-ED datasets are considered, allowing the universality of this structure solution strategy to be assessed.

The direct-space structure solution strategy is an impor-tant step forward to fully use the knowledge of reticular chemistry in facilitating the structure determination of COFs, even from low-resolution 3D-ED data.

Method

The direct-space strategy[14] for structure solution oper-ates by carrying out global optimization in direct space to find a structure that gives optimal agreement with experimental diffraction data. An important aspect underlying the success of the direct-space strategy is that the trial structures are defined by a suitable "structural fragment" constructed using reliably known information on molecular geometry (e.g. standard bond lengths, bond angles and geometries of rigid moieties such as aromatic rings). In general, trial crystal structures are defined by the position {x, y, z} and orientation {q, f, y} of the structural fragment relative to the unit cell axes, and the conformational geometry is specified by variable torsion angles {t_1, t_2, …, t_n}. The aim is to determine the global minimum on the R-factor hypersurface (i.e. R-factor as a function of the variables {x, y, z, q, f, y, t_1, t_2, …, t_n}).

In the present work, direct-space structure solution is implemented using a genetic algorithm[15] (GA) for global optimization, which effectively explores the R-factor hyper-surface by mimicking the processes of biological evolution. Starting from a randomly generated population of trial structures, the GA produces new structures by mating and mutation operations, and the population is allowed to evolve through a sequence of generations by natural selection. The GA is an implicitly parallel search of the R-factor hypersur-face, with different regions of structural space sampled simultaneously and with information swapped actively be-tween trial structures. In contrast, other global optimization algorithms[14] (such as SA or Monte Carlo) typically involve a sequential search to locate the global minimum. The parallel search strategy in the GA is conducive for efficiently locating the global minimum on the R-factor hypersurface, particu-larly when the number of structural variables is large.

Results and Discussion

The 3D-ED data were recorded for two phases of COF-300: an activated phase COF-300-V and a hydrated phase COF-300-H_2O, as discussed in our recent study of the dynamic behavior of COF-300 (Supporting Information, Section S1).[12g] For the COF-300-V sample, the 3D-ED data were recorded both at room temperature (COF-300-V-RT; Supporting Information, Figure S1) and using a cryogenic sample holder (COF-300-V-Cryo; Figure S1). For the COF-300-H_2O sample, the 3D-ED data were recorded using the cryogenic sample holder (COF-300-H_2O-Cryo; Figure S1). In each case, the unit cell (Supporting Information) and space group ($I4_1/a$) were determined from the 3D-ED data.

For the direct-space GA structure-solution calculations, appropriate structural variables must be defined. As COF materials have extended frameworks linked by covalent bonds, they do not contain discrete molecular entities that would allow the "structural fragment" to be defined straight-forwardly (as described for the case of molecular crystals under Method); thus, the COF framework must be consid-ered carefully in defining a suitable structural fragment for direct-space structure solution calculations. A starting point is to identify the asymmetric unit of the framework. Based on the synthetic protocol, COF-300 is known to be constructed from tetrahedral tetra-(4-anilyl)-methane building blocks and linear terephthaldehyde units, giving the structural fragment denoted "fragment-1" in Figure 2 a. The multiplicity of space group $I4_1/a$ is 16, with two special sites: 4-fold improper rotation axes (4) and inversion centers (1). The relatively small asymmetric unit and high space-group symmetry require that, to avoid molecular overlap, the building units should be compatible with 4 and/or 1 symmetry. The tetrahedral building block can achieve 4 symmetry with the central carbon located on a 4-site and, as the linear building units are centrosymmetric, the central benzene ring can be located on a 1 site. While the 4 symmetry element of $I4_1/a$ dictates that all fragment-1 units in the structure are symmetry-related, the 1 symmetry element of $I4_1/a$ dictates that fragment-1 has 1 symmetry. Thus, the asymmetric unit comprises half of fragment-1, as defined by "fragment-2" in Figure 2 b.

To solve the structure of COF-300 by direct-space structure solution, three different models were considered (Figure 2 c). In each model, the structural fragment includes all atoms in the asymmetric unit, with features of molecular geometry (bond lengths and bond angles) taken from similar

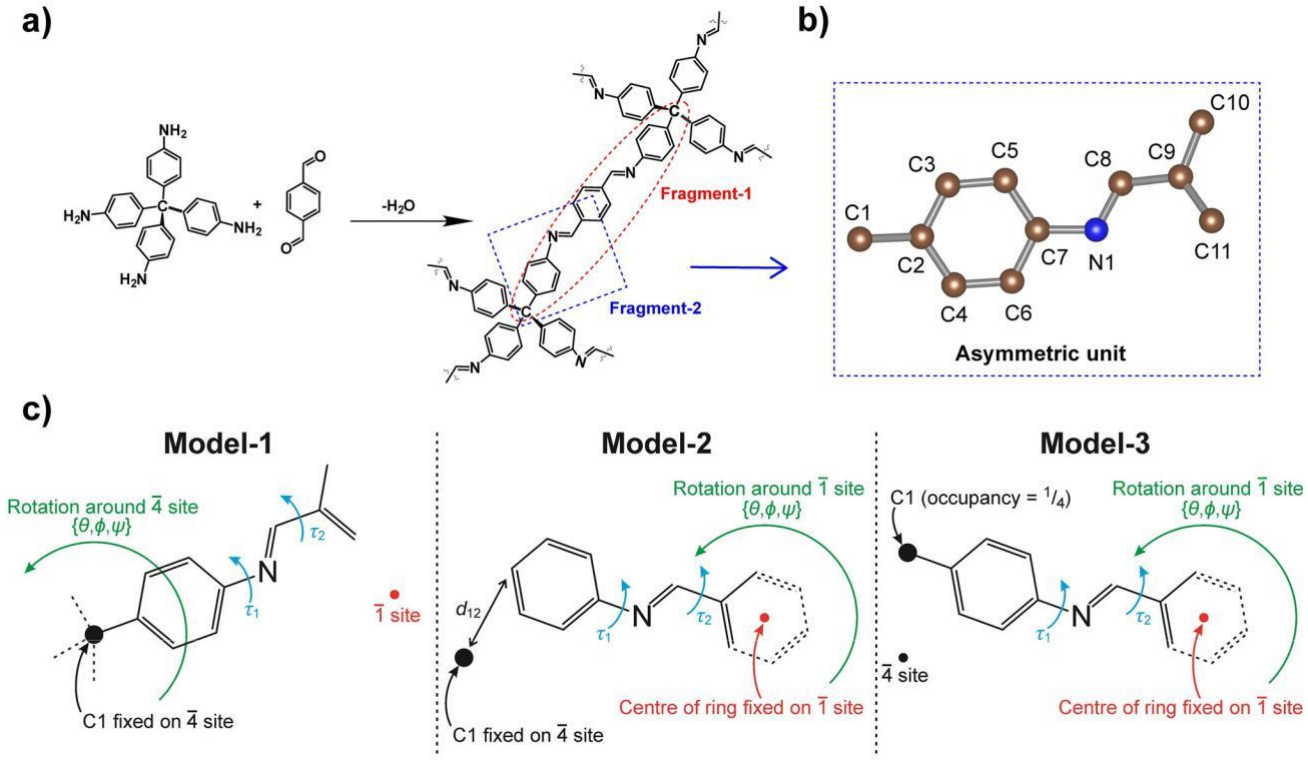

Figure 2. a) Construction of COF-300 from tetrahedral and linear building units. b) The asymmetric unit of COF-300 (corresponding to fragment-2 in (a)). c) Definition of the three structural models used in the direct-space GA structure solution calculations.

known structures (Supporting Information, Tables S1–3). From the above deductions, atom C1 in fragment-2 is located on a 4-site and the central benzene ring of the linear building unit is centered on a 1-site. On this basis, the structural variables for each model in the GA structure solution calculations can now be defined. In Model-1, C1 is fixed at a 4-site and the whole fragment is allowed to rotate freely (by variation of { , f, }) around the 4-site, with the conformation defined by two torsion-angle variables {t_1, t_2}. In Model-2, there are two independent sub-fragments formed by breaking the C1 C2 bond. The C1 atom is fixed on a 4-site while the central benzene ring of the other sub-fragment is fixed on a 1-site and allowed to rotate freely {q, f, y} around this site, with two variable torsion angles {t_1, t_2} defining the conformation. In Model-3, the central benzene ring is fixed on a 1-site and the whole fragment is allowed to rotate freely {q, f, y} around this site; the C1 atom is not constrained to be on a 4-site and the occupancy of C1 is fixed at 1/4 as this atom is shared by four symmetry-equivalent fragments (related by 4 symmetry). The conformation is defined by two variable torsion angles {t_1, t_2}.

All three models were used in EAGER calculations to find trial structures giving good agreement with the exper-imental 3D-ED data (i.e. low R-factor). However, low R-factor is not the only criterion for an acceptable structure solution, as it is possible (e.g. as a consequence of approx-imations inherent in the definition of the model and/or poor data quality) that some geometrically unreasonable structures could have low R-factor. Therefore, another essential crite-rion is that the structure must have acceptable geometric features, including the correct connectivity of the building units. Thus, the parts of the framework that were "broken" in defining the structural fragment must be "re-formed" with reasonable geometry to form the complete 3-dimensionally connected covalent framework. Also, the conformationally flexible parts in the structural fragment defined by variable torsion angles must have a reasonable geometry. Clearly, the criteria used to assess whether the structure solution is geometrically reasonable are different for each model. For Model-1, the central benzene ring must be successfully formed by an appropriate connection between two symmetry-related structural fragments around the 1-site. For Model-2, the distance between C1 and C2 (denoted d_{12} in Figure 2 c) must correspond to a covalent bond with acceptable bond length. For Model-3, as the occupancy of C1 is fixed at 1/4, a successful structure solution must have the C1 atoms of four symmetry-related structural fragments superimposed (at least approximately) on the 4-site. For each model, the expectation is that the structure solution must be sufficiently close to the correct structure to be able to converge to the correct structure in subsequent structure refinement (e.g. Rietveld refinement using PXRD data or geometry optimization using DFT-D calculations).

To assess the quality of structure solutions obtained in the direct-space GA calculations, we focus on the results for the COF-300-V-Cryo and COF-300-H_2O-Cryo datasets (Sec-tion S2). For COF-300-V-Cryo (Figures S1 and S2), all three models give structure solutions that correspond to the correct covalently connected framework, with all the "broken" parts of the structure re-formed successfully (Figures 3 a–c;

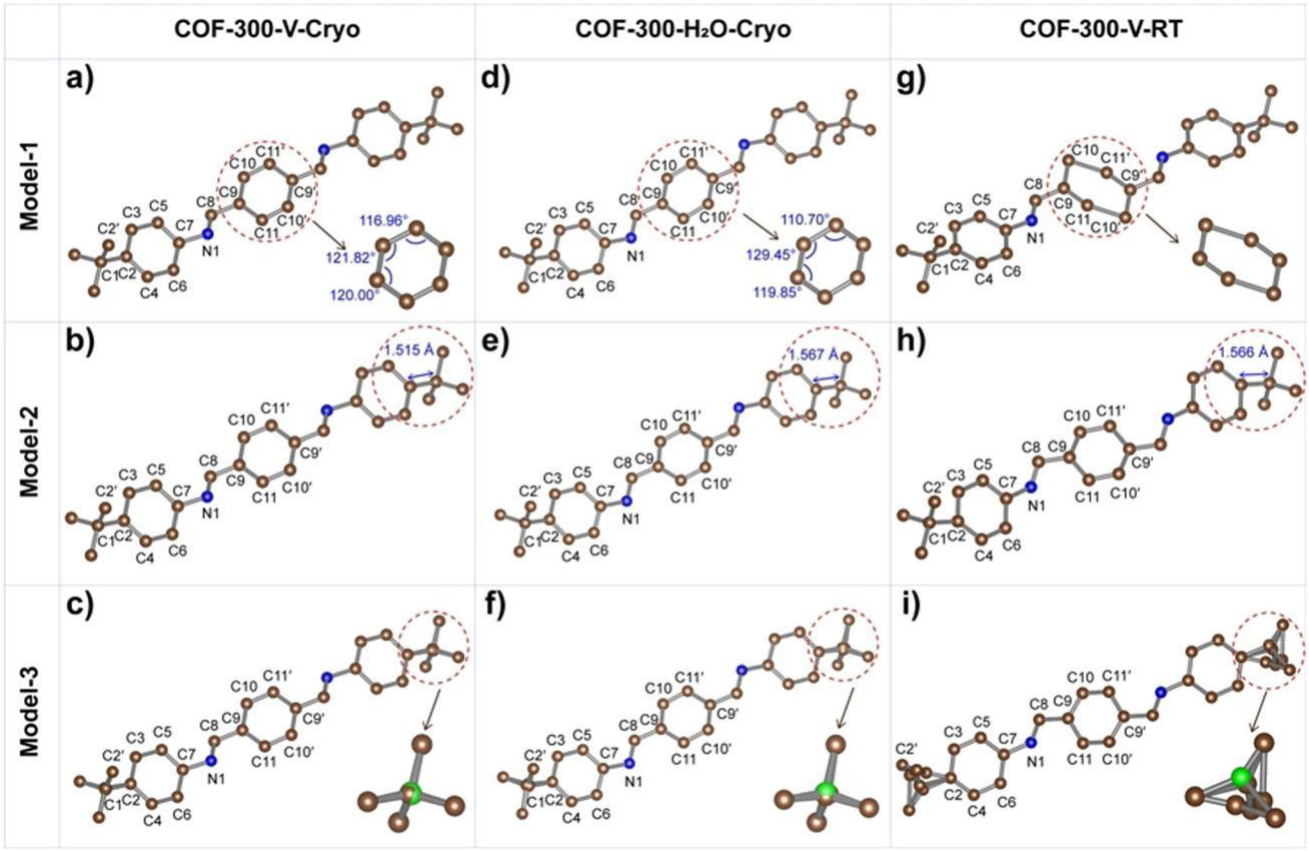

Figure 3. Results from direct-space GA structure-solution calculations using Model-1 (top), Model-2 (middle) and Model-3 (bottom) for the following 3D-ED datasets: a–c) COF-300-V-Cryo, d–f) COF-300-H_2O-Cryo, and g–i) COF-300-V-RT. In each case, the best structure solution obtained using each model is shown.

Tables S4–S6). For Model 1, the central benzene ring is re-formed at the 1-site with reasonable geometry. For Model-2, the C1 C2 bond is re-formed with acceptable bond length (d_{12} = 1.52 &) and the torsion angles in the best trial structure are acceptably close to the reported structure[12g] (Table S2). For Model-3, the C1 atoms of the four symmetry related fragments are very close to the 4-site and the variable torsion angles are reasonable. For COF-300-H_2O-Cryo (Figures S1 and S2), structure solution is again successful for all three models (Figures 3 d–f). For Model-1, the central benzene ring is re-formed with reasonable geometry; for Model-2, the C1 C2 bond is re-formed successfully (d_{12} = 1.57 &); for Model-3, the C1 atoms of the four symmetry related fragments are very close (0.09 &) to the 4-site. However, Model-2 and Model-3 perform better than Model-1 in terms of the torsion angles in the best trial structure (Tables S7–S9). GA structure-solution calculations were also carried out for COF-300-H_2O-Cryo using each model defined in Figure 2 c but with a single oxygen atom added to the model (allowed to translate freely {x, y, z} in the unit cell) to represent the water molecules in the structure. Significantly, in the best structure solution for each model, this oxygen atom is located at the correct site in the channel of the COF-300 framework (Figure S3).

Direct-space GA structure-solution calculations using all three models were then carried out for the COF-300-V-RT dataset. Compared to the other two datasets, the quality of COF-300-V-RT is rather poor, with lower resolution (1.1 &) and fewer reflections (completeness 38 %), attributed to electron beam damage and thermal effects (Figure 1; Fig-ure S2). Significantly, previous attempted structure solution using traditional direct methods and charge flipping on this dataset were unsuccessful,[12g] as only the position of the central carbon atom of the tetrahedral building unit was resolved (Figure S4). In the direct-space GA structure solution calculations using the full COF-300-V-RT dataset, a structure solution of acceptable quality was obtained only for Model-2 (Figures 3 g–i). For Model-1, although the central benzene ring is recognizable, the geometry of this ring deviates from reasonable bond lengths and bond angles (Tables S10–S12). For Model-3, the four symmetry-related C1 atoms that should converge on the 4-site are rather far (0.56 &) from the 4-site.

Given the better performance of Model-2 in GA structure solution calculations on the full COF-300-V-RT dataset, structure solution using Model-2 was also carried out on resolution-limited 3D-ED datasets containing only a subset of the reflections in COF-300-V-RT (Section S3). The resolu-tion-limited datasets were generated by excluding all reflec-tions with q greater than a specified maximum value (q_{max}), with q_{max} ranging from 0.15**8** to 0.625**8** [the corresponding resolution is given by $d = l/(2 \sin q_{max})$, with l = 0.02508 &; Table 1; Tables S13–S15]. GA structure-solution calculations

Table 1: Results from direct-space GA structure-solution calculations using Model-2 on the resolution-limited datasets derived from the full experimental COF-300-V-RT dataset (for further details see Section S3).

q_{max} [Å][a]	Resolution [Å]	No. of peaks[b]	Quality[c]	d_{12} [Å][d]	a_{123} [°][d]	a_{124} [°][d]	t_1 [°][d]	t_2 [°][d]	t_3 [°][d]
0.15	4.79	10	Low	1.92	91.5	142.6	50.7	145.6	52.0
0.16	4.49	12	Low	1.89	148.6	87.1	24.4	163.7	89.9
0.17	4.23	13	Low	1.88	150.3	85.9	18.6	156.6	155.8
0.18	3.99	14	Low	1.82	152.0	86.1	22.8	156.1	147.0
0.19	3.78	18	High*	1.55	121.0	118.1	56.4	159.2	97.9
0.20	3.59	22	High*	1.51	128.3	111.8	42.2	169.0	107.9
0.21	3.42	23	High*	1.51	126.1	113.9	46.0	174.6	107.1
0.225	3.19	31	High	1.54	119.1	120.1	56.0	156.9	98.1
0.25	2.87	39	High	1.51	126.5	113.5	48.2	175.0	109.4

[a] Results are only shown for calculations with q_{max} 0.25Å; calculations with higher q_{max} (0.375Å, 0.50Å, 0.625Å) all give high-quality structure solutions comparable to that obtained for the full COF-300-V-RT dataset. [b] Number of independent reflections. [c] Quality of the best structure solution, based on the geometric criteria discussed in the text (in those cases marked with an asterisk, the trial structure with the most reasonable geometric features has an R-factor slightly higher than the trial structure of lowest R-factor; Figure S5). [d] Geometric properties of the best structure solution: d_{12} =C1 C2 distance (Figure 2 c), a_{123} = C1-C2-C3 angle, a_{124} =C1-C2-C4 angle, t_1 = C5-C7-N1-C8 torsion angle, t_2 =N1-C8-C9-C10 torsion angle, t_3 =C2'-C1-C2-C3 torsion angle.

using Model-2 were carried out on each resolution-limited dataset to establish whether geometrically reasonable structure solutions are obtained, as judged by the following criteria: the C1 C2 bond distance (d_{12} in Table 1) is in the range (1.54 0.05) Å, the C1-C2-C3 and C1-C2-C4 bond angles (a_{123} and a_{124} in Table 1) are in the range (120 10)° and the C5-C7-N1-C8, N1-C8-C9-C10 and C2'-C1-C2-C3 torsion angles (t_1, t_2 and t_3 in Table 1) are acceptably close (within ca. 20°) to those in the reported structure[12g] (t_1 = 49.6°; t_2 = 167.9°; t_3 = 100.7°). Based on these criteria, "high-quality" structure solutions were achieved for all datasets with q_{max} 0.19Å (Table 1; Tables S16–S25), giving geometrically reasonable structures with a complete framework and correct interpenetration number (Figures S5–S7).

We note that the dataset with q_{max} = 0.19Å (resolution 3.78 Å) contains only 18 independent reflections.

For q_{max} 0.19Å, the re-formed C1 C2 bond length in the structure solution is in the range (1.54 0.03) Å, close to the optimal value, the C1-C2-C3 and C1-C2-C4 angles are close to the ideal value of 120°, and the torsion angles are also reasonable (Table 1). For the datasets at lower resolution (q_{max} < 0.19Å), the best structure solution deviates from standard geometric features, although it may still be sufficiently close to the correct structure to allow subsequent refinement (e.g. Rietveld refinement on PXRD data, or DFT-D geometry optimization) to converge to the correct structure. The 3D electrostatic potential maps calculated for trial structures may also provide valuable insights in the structure determination process (Figure S8).

Conclusion

We have shown that the crystal structure of COF-300 can be solved successfully from low-resolution 3D-ED data using the direct-space GA technique for structure solution, thus validating an approach that may be applied for structure solution of other COF materials when only low-resolution 3D-ED data are available. The strategy requires knowledge of reticular chemistry and handling of nanocrystals, together with the application of model building strategies and reliable structure solution from the 3D-ED data using a direct-space method. Significantly, we have shown that this strategy can achieve successful structure solution from very low-resolution 3D-ED data (with resolution as low as 3.78 Å). Given the difficulty of preparing COF materials suitable for single-crystal XRD, this strategy has considerable potential to overcome the challenge of solving the structures of sub-micrometer-sized COF crystals with relatively low crystallinity.

Acknowledgements

This work is supported by the National Natural Science Foundation of China (No. 21875140, 21835002, 21522105 and 51861145313). The authors thank Prof. Osamu Terasaki and ChEM SPST, ShanghaiTech University (#EM02161943), for scientific and characterization support. K.D.M.H. is grateful to ShanghaiTech University for an appointment as a Distinguished Adjunct Professor. We thank Supercomputing Wales for access to computational facilities.

Conflict of interest

The authors declare no conflict of interest.

Keywords: 3D electron diffraction · direct space structure solution · genetic algorithms · low resolution

[1] a) O. M. Yaghi, M. J. Kalmutzki, C. S. Diercks, Introduction to Reticular Chemistry: Metal Organic Frameworks and Covalent Organic Frameworks, Wiley-VCH, Weinheim, 2019, p. 509; b) A. P. C,t , A. I. Benin, N. W. Ockwig, M. O Keeffe, A. J. Matzger, O. M. Yaghi, Science 2005, 310, 1166 – 1170; c) H. M. El-Kaderi, J. R. Hunt, J. Mendoza-Cortes, A. P. Cote, R. Taylor, M. O Keeffe, O. M. Yaghi, Science 2007, 316, 268 – 272; d) Y. Liu, Y. Ma, Y. Zhao, X. Sun, F. GQndara, H. Furukawa, Z. Liu, H. Zhu, C. Zhu, K. Suenaga, P. Oleynikov, A. S. Alshammari, X. Zhang, O. Terasaki, O. M. Yaghi, Science 2016, 351, 365 – 369; e) C. S. Diercks, O. M. Yaghi, Science 2017, 355, eaal1585.

[2] a) K. Geng, T. He, R. Liu, S. Dalapati, K. T. Tan, Z. Li, S. Tao, Y. Gong, Q. Jiang, D. Jiang, Chem. Rev. 2020, 120, 8814 – 8933; b) X. Guan, F. Chen, Q. Fang, S. Qiu, Chem. Soc. Rev. 2020, 49, 1357 – 1384.

[3] a) H. Ning, W. Ping, J. Donglin, Nat. Rev. Mater. 2016, 1, 16068; b) X. Han, C. Yuan, B. Hou, L. Liu, H. Li, Y. Liu, Y. Cui, Chem. Soc. Rev. 2020, https://doi.org/10.1039/D0CS00009D.

[4] a) X. Guan, H. Li, Y. Ma, M. Xue, Q. Fang, Y. Yan, V. Valtchev, S. Qiu, Nat. Chem. 2019, 11, 587 – 594; b) Y. Jin, Y. Hu, W. Zhang, Nat. Rev. Chem. 2017, 1, 0056; c) Y. Song, Q. Sun, B. Aguila, S. Ma, Adv. Sci. 2019, 6, 1801410; d) S. Kandambeth, K. Dey, R. Banerjee, J. Am. Chem. Soc. 2019, 141, 1807 – 1822; e) S. Ding, W. Wang, Chem. Soc. Rev. 2013, 42, 548 – 568; f) L. Zhu, Y.-B. Zhang, Molecules 2017, 22, 1149; g) D. D. Medina, T. Sick, T. Bein, Adv. Energy Mater. 2017, 7, 1700387; h) J. Li, X. Jing, Q. Li, S. Li, X. Gao, X. Feng, B. Wang, Chem. Soc. Rev. 2020, 49, 3565 – 3604; i) Z. Wang, S. Zhang, Y. Chen, Z. Zhang, S. Ma, Chem. Soc. Rev. 2020, 49, 708 – 735.

[5] T. Ma, E. A. Kapustin, S. X. Yin, L. Liang, Z. Zhou, J. Niu, L.-H. Li, Y. Wang, J. Su, J. Li, X. Wang, W. D. Wang, W. Wang, J. Sun, O. M. Yaghi, Science 2018, 361, 48 – 52.

[6] a) J. R. Hunt, C. J. Doonan, J. D. LeVangie, A. P. Cote, O. M. Yaghi, J. Am. Chem. Soc. 2008, 130, 11872 – 11873; b) Q. R. Fang, J. H. Wang, S. Gu, R. B. Kaspar, Z. B. Zhuang, J. Zheng, H. X. Guo, S. L. Qiu, Y. S. Yan, J. Am. Chem. Soc. 2015, 137, 8352 – 8355; c) G. Q. Lin, H. M. Ding, D. Q. Yuan, B. S. Wang, C. Wang, J. Am. Chem. Soc. 2016, 138, 3302 – 3305; d) Y. X. Ma, Z. J. Li, L. Wei, S. Y. Ding, Y. B. Zhang, W. Wang, J. Am. Chem. Soc. 2017, 139, 4995 – 4998; e) C. Wang, Y. Wang, R. L. Ge, X. D. Song, X. Q. Xing, Q. K. Jiang, H. Lu, C. Hao, X. W. Guo, Y. A. Gao, D. L. Jiang, Chem. Eur. J. 2018, 24, 585 – 589; f) P. X. Guan, J. K. Qiu, Y. L. Zhao, H. Y. Wang, Z. Y. Li, Y. L. Shi, J. J. Wang, Chem. Commun. 2019, 55, 12459 – 12462.

[7] a) D. L. Dorset, Ultramicroscopy 2007, 107, 453 – 461; b) P. Wagner, O. Terasaki, S. Ritsch, J. G. Nery, S. I. Zones, M. E. Davis, K. Hiraga, J. Phys. Chem. B 1999, 103, 8245 – 8250; c) L. Palatinus, P. BrQzda, P. Boullay, O. Perez, M. KlementovQ, S. Petit, V. Eigner, M. Zaarour, S. Mintova, Science 2017, 355, 166 – 169; d) T. Willhammar, Y. Yun, X. Zou, Adv. Funct. Mater. 2014, 24, 182 – 199; e) Y. Ma, P. Oleynikov, O. Terasaki, Nat. Mater. 2017, 16, 755 – 759; f) Y. Ma, L. Han, Z. Liu, A. Mayoral, I. D%az, P. Oleynikov, T. Ohsuna, Y. Han, M. Pan, Y. Zhu, Y. Sakamoto, S. Che, O. Terasaki in Springer Handbook of Microscopy (Eds.: P. W. Hawkes, J. C. H. Spence), Springer International Publishing, Cham, 2019, pp. 2-2.

[8] a) U. Kolb, T. Gorelik, C. K4bel, M. T. Otten, D. Hubert, Ultramicroscopy 2007, 107, 507 – 513; b) D. Zhang, P. Oleynikov, S. Hovmçller, X. Zou, Z. Kristallogr. 2010, 225, 94 – 102; c) D. Shi, B. L. Nannenga, M. G. Iadanza, T. Gonen, eLife 2013, 2, e01345; d) W. Wan, J. Sun, J. Su, S. Hovmçller, X. Zou, J. Appl. Crystallogr. 2013, 46, 1863 – 1873; e) M. Gemmi, P. Oleynikov, Z. Kristallogr. 2013, 228, 51 – 58; f) L. N. Brent, S. Dan, G. W. L. Andrew, G. Tamir, Nat. Methods 2014, 11, 927 – 930; g) M. Gemmi, M. G. I. La Placa, A. S. Galanis, E. F. Rauch, S. Nicolopoulos, J. Appl. Crystallogr. 2015, 48, 718 – 727; h) Y. Wang, T. Yang, H. Xu, X. Zou, W. Wan, J. Appl. Crystallogr. 2018, 51, 1094 – 1101.

[9] a) E. Mugnaioli, U. Kolb, Microporous Mesoporous Mater. 2014, 189, 107 – 114; b) P. Guo, J. Shin, A. G. Greenaway, J. G. Min, J. Su, H. J. Choi, L. Liu, P. A. Cox, S. B. Hong, P. A. Wright, X. Zou, Nature 2015, 524, 74 – 78; c) J. Simancas, R. Simancas, P. J. Bereciartua, J. L. Jorda, F. Rey, A. Corma, S. Nicolopoulos, P. Pratim Das, M. Gemmi, E. Mugnaioli, J. Am. Chem. Soc. 2016, 138, 10116 – 10119; d) M. Feyand, E. Mugnaioli, F. Vermoortele, B. Bueken, J. M. Dieterich, T. Reimer, U. Kolb, D. De Vos, N. Stock, Angew. Chem. Int. Ed. 2012, 51, 10373 – 10376; Angew. Chem. 2012, 124, 10519 – 10522; e) B. Wang, T. Rhauderwiek, A. K. Inge, H. Xu, T. Yang, Z. Huang, N. Stock, X. Zou, Chem. Eur. J. 2018, 24, 17429 – 17433; f) D. Denysenko, M. Grzywa, M. Tonigold, B. Streppel, I. Krkljus, M. Hirscher, E. Mugnaioli, U. Kolb, J. Hanss, D. Volkmer, Chem. Eur. J. 2011, 17, 1837 – 1848; g) S. Leubner, V. Bengtsson, A. Inge, M. Wahiduzzaman, F. Steinke, A. Jaworski, S. Halis, P. Rçnfeldt, H. Reinsch, G. Maurin, X. Zou, N. Stock, Dalton Trans. 2020, 49, 3088 – 3092.

[10] a) E. van Genderen, M. T. B. Clabbers, P. P. Das, A. Stewart, I. Nederlof, K. C. Barentsen, Q. Portillo, N. S. Pannu, S. Nicolopoulos, T. Gruene, J. P. Abrahams, Acta Crystallogr. 2016, 72, 236 – 242; b) T. Gruene, J. T. C. Wennmacher, C. Zaubitzer, J. J. Holstein, J. Heidler, A. Fecteau-Lefebvre, S. De Carlo, E. M4ller, K. N. Goldie, I. Regeni, T. Li, G. Santiso-Quinones, G. Steinfeld, S. Handschin, E. Van Genderen, J. A. van Bokhoven, G. H. Clever, R. Pantelic, Angew. Chem. Int. Ed. 2018, 57, 16313 – 16317; Angew. Chem. 2018, 130, 16551 – 16555; c) P. P. Das, E. Mugnaioli, S. Nicolopoulos, C. Tossi, M. Gemmi, A. Galanis, G. Borodi, M. M. Pop, Org. Process Res. Dev. 2018, 22, 1365 – 1372; d) C. G. Jones, M. W. Martynowycz, J. Hattne, T. J. Fulton, B. M. Stoltz, J. A. Rodriguez, H. M. Nelson, T. Gonen, ACS Cent. Sci. 2018, 4, 1587 – 1592; e) H. Zhou, F. Luo, Z. Luo, D. Li, C. Liu, X. Li, Anal. Chem. 2019, 91, 10996 – 11003.

[11] a) K. Yonekura, K. Kato, M. Ogasawara, M. Tomita, C. Toyoshima, Proc. Natl. Acad. Sci. USA 2015, 112, 3368 – 3373; b) J. A. Rodriguez, M. I. Ivanova, M. R. Sawaya, D. Cascio, F. E. Reyes, D. Shi, S. Sangwan, E. L. Guenther, L. M. Johnson, M. Zhang, L. Jiang, M. A. Arbing, B. L. Nannenga, J. Hattne, J. Whitelegge, A. S. Brewster, M. Messerschmidt, S. Boutet, N. K. Sauter, T. Gonen, D. S. Eisenberg, Nature 2015, 525, 486; c) F. Luo, X. Gui, H. Zhou, J. Gu, Y. Li, X. Liu, M. Zhao, D. Li, X. Li, C. Liu, Nat. Struct. Mol. Biol. 2018, 25, 341 – 346; d) S. Liu, T. Gonen, Commun. Biol. 2018, 1, 38; e) H. Xu, H. Lebrette, T. Yang, V. Srinivas, S. Hovmçller, M. Hçgbom, X. Zou, Structure 2018, 26, 667 – 675.e663; f) D. Li, C. Liu, Biochemistry 2020, 59, 639 – 646.

[12] a) Y. B. Zhang, J. Su, H. Furukawa, Y. Yun, F. Gandara, A. Duong, X. Zou, O. M. Yaghi, J. Am. Chem. Soc. 2013, 135, 16336 – 16339; b) T. Ma, J. Li, J. Niu, L. Zhang, A. S. Etman, C. Lin, D. Shi, P. Chen, L. H. Li, X. Du, J. Sun, W. Wang, J. Am. Chem. Soc. 2018, 140, 6763 – 6766; c) Y. Liu, Y. Ma, J. Yang, C. S. Diercks, N. Tamura, F. Jin, O. M. Yaghi, J. Am. Chem. Soc. 2018, 140, 16015 – 16019; d) H. Ding, J. Li, G. Xie, G. Lin, R. Chen, Z. Peng, C. Yang, B. Wang, J. Sun, C. Wang, Nat. Commun. 2018, 9, 5234; e) Y. Liu, C. S. Diercks, Y. Ma, H. Lyu, C. Zhu, S. A. Alshmimri, S. Alshihri, O. M. Yaghi, J. Am. Chem. Soc. 2019, 141, 677 – 683; f) C. Gao, J. Li, S. Yin, G. Lin, T. Ma, Y. Meng, J. Sun, C. Wang, Angew. Chem. Int. Ed. 2019, 58, 9770 – 9775; Angew. Chem. 2019, 131, 9872 – 9877; g) T. Sun, L. Wei, Y. Chen, Y. Ma, Y. B. Zhang, J. Am. Chem. Soc. 2019, 141, 10962 – 10966; h) L. Zhang, Y. Zhou, M. Jia, Y. He, W. Hu, Q. Liu, J. Li, X. Xu, C. Wang, A. Carlsson, S. Lazar, A. Meingast, Y. Ma, J. Xu, W. Wen, Z. Liu, J. Cheng, H. Deng, Matter 2020, 2, 1 – 15; i) H.-S. Xu, Y. Luo, X. Li, P. Z. See, Z. Chen, T. Ma, L. Liang, K. Leng, I. Abdelwahab, L. Wang, R. Li, X. Shi, Y. Zhou, X. F. Lu, X. Zhao, C. Liu, J. Sun, K. P. Loh, Nat. Commun. 2020, 11, 1434; j) C. Gao, J. Li, S. Yin, J. Sun, C. Wang, J. Am. Chem. Soc. 2020, 142, 3718 – 3723; k) T. Sun, L. Wei, Y. Ma, Y. B. Zhang, Chin. J. Chem. 2020, 38, 1153 – 1166.

[13] R. Cerný, V. Favre-Nicolin, Z. Kristallogr. 2007, 222, 105 – 113.

[14] a) K. D. M. Harris, M. Tremayne, P. Lightfoot, P. G. Bruce, J. Am. Chem. Soc. 1994, 116, 3543 – 3547; b) H. Tsue, M. Horiguchi, R. Tamura, K. Fujii, H. Uekusa, J. Synth. Org. Chem. Jpn. 2007, 65, 1203 – 1212; c) W. I. F. David, K. Shankland, Acta Crystallogr. Sect. A 2008, 64, 52 – 64; d) K. D. M. Harris, Top. Curr. Chem. 2011, 315, 133 – 177.

[15] a) B. M. Kariuki, H. Serrano-GonzQlez, R. L. Johnston, K. D. M. Harris, Chem. Phys. Lett. 1997, 280, 189 – 195; b) K. Shankland, W. I. F. David, T. Csoka, Z. Kristallogr. 1997, 212, 550 – 552; c) K. D. M. Harris, R. L. Johnston, B. M. Kariuki, Acta Crystallogr. Sect. A 1998, 54, 632 – 645; d) Z. J. Feng, C. Dong, J. Appl. Crystallogr. 2007, 40, 583 – 588.

[16] Y. Chen, Z. L. Shi, L. Wei, B. Zhou, J. Tan, H. L. Zhou, Y. B. Zhang, J. Am. Chem. Soc. 2019, 141, 3298 – 3303.

[17] a) K. D. M. Harris, R. L. Johnston, C. E. Hughes, Z. Zhou, S. Habershon, G. W. Turner, P. A. Williams, B. M. Kariuki, E. Y. Cheung, EAGER—A Computer Program for Direct-Space Structure Solution from Diffraction Data, Cardiff University; b) K. D. M. Harris, R. L. Johnston, S. Habershon, Struct. Bonding (Berlin) 2004, 110, 55 – 94; c) K. D. M. Harris, S. Habershon, E. Y. Cheung, R. L. Johnston, Z. Kristallogr. 2004, 219, 838 – 846.

[18] a) B. M. Kariuki, P. Calcagno, K. D. M. Harris, D. Philp, R. L. Johnston, Angew. Chem. Int. Ed. 1999, 38, 831 – 835; Angew. Chem. 1999, 111, 860 – 864; b) D. Albesa-Jov , B. M. Kariuki, S. J. Kitchin, L. Grice, E. Y. Cheung, K. D. M. Harris, ChemPhysChem 2004, 5, 414 – 418; c) F. Guo, J. Mart%-Rujas, Z. Pan, C. E. Hughes, K. D. M. Harris, J. Phys. Chem. C 2008, 112, 19793 – 19796; d) P. A. Williams, C. E. Hughes, G. K. Lim, B. M. Kariuki, K. D. M. Harris, Cryst. Growth Des. 2012, 12, 3104 – 3113; e) J. Mart%-Rujas, L. Meazza, G. K. Lim, G. Terraneo, T. Pilati, K. D. M. Harris, P. Metrangolo, G. Resnati, Angew. Chem. Int. Ed. 2013, 52, 13444 – 13448; Angew. Chem. 2013, 125, 13686 – 13690; f) C. E. Hughes, G. N. M. Reddy, S. Masiero, S. P. Brown, P. A. Williams, K. D. M. Harris, Chem. Sci. 2017, 8, 3971 – 3979; g) O. Al Rahal, C. E. Hughes, P. A. Williams, A. J. Logsdail, Y. Diskin-Posner, K. D. M. Harris, Angew. Chem. Int. Ed. 2019, 58, 18788 – 18792; Angew. Chem. 2019, 131, 18964 – 18968; h) I. Brekalo, W. Yuan, C. Mottillo, Y. Lu, Y. Zhang, J. Casaban, K. T. Holman, S. L. James, F. Duarte, P. A. Williams, K. D. M. Harris, T. Fris˘c˘ic´, Chem. Sci. 2020, 11, 2141 – 2147.